

# The effect of the strain relaxation in InAs/GaAs stacked quantum dots and multiple quantum wells on the Raman spectrum

Olga L. Lazarenkova<sup>1</sup>, Paul von Allmen<sup>1</sup>, Seungwon Lee<sup>1</sup>, Fabiano Oyafuso<sup>1</sup>, and Gerhard Klimeck<sup>1,2</sup>

<sup>1</sup> Jet Propulsion Laboratory, California Inst. of Techn., 4800 Oak Grove Dr. MS: 169-315, Pasadena CA 91109, USA

<sup>2</sup> Purdue University, Network for Computational Nanotechnology, Electrical Engineering, W. Lafayette, IN 47906, USA

**Abstract.** Atomistic-level simulations of the Raman shift in InAs/GaAs multiple quantum well (MQW) and stacked quantum dot (SQD) structures as a function of interlayer separation are reported. The simulations utilize an augmented Keating model which includes anharmonicity corrections. It is demonstrated that the interaction between angle distorted bonds is responsible for the penetration of the strain into the GaAs barrier. This result is in contrast to a complete strain relaxation of the GaAs barrier which would be predicted by *continuum models*. Tension along the growth direction result in the red shift of the GaAs LO Raman peak as the barrier thickness decreases in both, MQW and SQD, structures.

Understanding the driving forces for the stacked quantum dot (SQD) formation, the resulting strain-modified optical properties and vibrational modes is of critical importance for sensor application of nanostructures. The class of highly strained self-assembled InAs/GaAs nanostructures are of particular interest for optical sensor applications. For such structures Raman spectroscopy can provide useful information on the built-in strain.

Within a computational model the total strain energy in the whole system must be minimized. The most widely used atomistic-level model for the calculation of the strain energy in the harmonic approximation is the two-parameter Valence-Force-Field (VFF) Keating model [1], later modified by Martin [2]. Atoms on a crystal lattice are treated as points connected by springs. Atomic bond stretching and bond angle changes are included through two separate terms with corresponding VFF “spring” constants. We have previously [3] introduced the anharmonicity of the interatomic potential into those constants.

The proper parameterization of the Keating model is of critical importance for the simulation of the strain effects on the GaAs LO phonon Raman shift in InAs/GaAs nanostructures. The VFF constants in *unstrained* materials are taken from Ref. [4]. The “shear deformation” anharmonicity correction was found from the experimental shear deformation parameter [5], which describes the corresponding shift of the optical phonon energy in the bulk crystal. The choice of the “hydrostatic” anharmonicity parameters both for bond stretching and bond bending terms was made by fitting to the experimental values [6] of the Grüneisen coefficients (Table 1), describing the dependence of the frequency of the phonon vibrations on the change of volume. This model is *not complete enough* to *simultaneously* model the strain dependence of the acoustic and optical phonon spectra. To avoid further model complications by the introduction of additional parameters we use two distinct parameter sets for different computational targets. The first “acoustical set” works better for the deformations of the long-wave acoustical type and is used for the strain energy minimization. The second “optical set” describes the optical phonons in the deformed structures (Table 1) better. Note that despite its shortcomings our model is a significant improvement over the standard Keating model, which fails to reproduce the

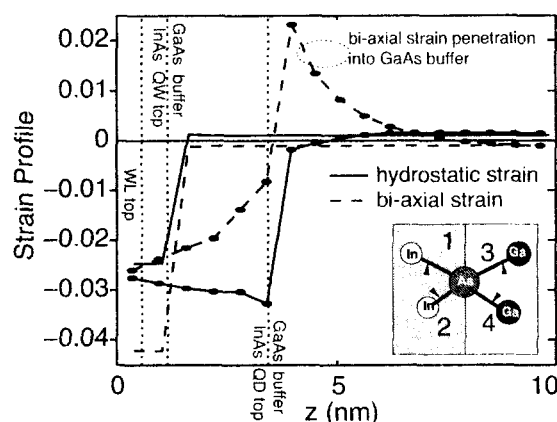


**Fig. 1.** Strain comparison along the growth direction in QDs (lines with dots) and QWs. Hydrostatic strain in solid lines and bi-axial in dashed lines. The vertical dotted lines mark the InAs/GaAs transitions of WL, QW, and the top of QD. The inset shows the scheme of the penetration of the deformation into GaAs barriers from InAs QW lattice matched to GaAs.

The devices considered in this work are based on InAs structures grown on a GaAs substrate. Two different structures are considered in particular: 1) infinitely flat QD, i.e., the structure equivalent to MQW, and 2) semi-spherical QDs on a wetting layer (WL). Both structures have the same mass of InAs. Continuum theory predicts the complete strain relaxation in the GaAs barrier in MQW grown on GaAs substrate and bi-axially strained InAs QWs. In contrast, atomistic treatment of the interaction between InAs (atoms 1 and 2 on the inset in Fig. 1) and GaAs bonds (atoms 3 and 4) leads to the deviation from the equilibrium of the angle between GaAs bonds. Bond angle deformation results in the penetration of nonzero bi-axial and hydrostatic strain in both, InAs and GaAs, materials (Fig. 1).

The strain penetration from the InAs structure into the GaAs buffer depends on the GaAs buffer size that separates subsequent quantum dot and quantum well layers. Fig. 2 analyzes the interlayer distance and quantum strain dependence. The pure bi-axial strain of InAs layer grown on GaAs is the limiting case of infinitesimal width of the layer (Fig. 2a). Even though the average strain in the barrier vanishes at large interlayer separations (Fig. 2b), some amount of GaAs adjacent to InAs remains bi-axially strained. This area

**Table 1.** Grüneisen parameters for GaAs and InAs computed within two-parameter Keating model (K) and including acoustical (AA) and optical (OA) sets of anharmonicity corrections in comparison with experimental values from Ref. [6]. The relative error  $\delta$  in per cent is shown where applicable. “F” indicates failure to reproduce the sign of the Grüneisen coefficient.

	$\gamma_K^{GaAs}$	$\delta\%$	$\gamma_{AA}^{GaAs}$	$\delta\%$	$\gamma_{OA}^{GaAs}$	$\delta\%$	$\gamma_{exp}^{GaAs}$	$\gamma_K^{InAs}$	$\delta\%$	$\gamma_{AA}^{InAs}$	$\delta\%$	$\gamma_{OA}^{InAs}$	$\delta\%$	$\gamma_{exp}^{InAs}$
$\gamma_{TA}^\Gamma$	-1.6591	F	0.5280	-0.5	0.5393	1.5	0.531	-2.0610	F	0.1435	2.5	0.1389	-0.7	0.14
$\gamma_{LA}^\Gamma$	-0.9937	F	1.3031	0.008	0.8659	-33	1.303	-1.0264	F	1.3902	0.7	0.6842	-51	1.4
$\gamma_{TA}^X$	-1.4147	-13	0.7237	F	0.8659	F	-1.62	-1.8484		0.3182		0.4690		
$\gamma_{LA}^X$	-0.6576		1.6618		1.2815			-0.6963		1.7569		0.9414		
$\gamma_{TO}^\Gamma$	-0.6560	F	1.6965	88	1.2230	36	0.9	-0.6992	F	1.7886	110	0.8459	-0.5	0.85
$\gamma_{LO}^\Gamma$	-0.6560	F	1.6965	22	1.2230	-12	1.39							
$\gamma_{TO}^X$	-0.6560	F	1.6965	38	1.2230	-0.5	1.23	-0.6992		1.7886		0.8459		
$\gamma_{LO}^X$	-0.5698	F	1.8344	6	1.2278	-29	1.73	-0.5862		1.9560		0.8493		
$\gamma_{LO}^X$	-0.6563		1.6618		1.2809			-0.6998		1.7527		0.9412		

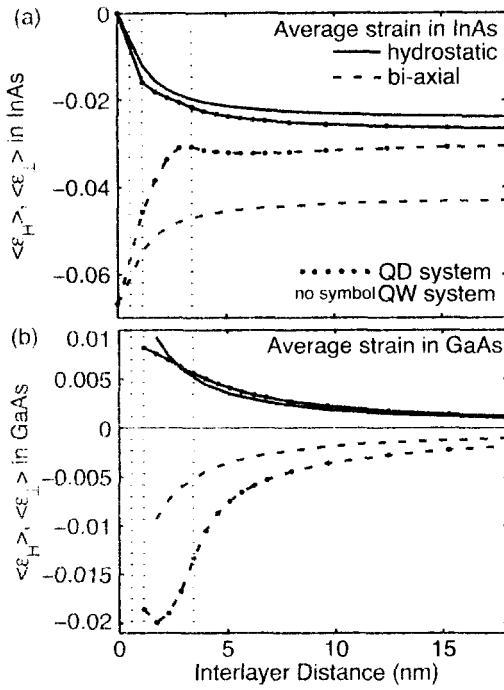


**Fig. 2.** Average hydrostatic ( $\langle \epsilon_H \rangle$ ) (solid lines) and bi-axial ( $\langle \epsilon_\perp \rangle$ ) (dashed lines) components of the strain inside (a) InAs and (b) GaAs materials in InAs/GaAs MQW and semi-spherical SQD (lines marked with dots) structures as a function of the interlayer distance. The vertical dotted lines mark the width of WL, QW, and the top of QD on WL.

phonons, resulting in the blue Raman shift (Fig. 3). At closer separation of InAs layers the hydrostatic tension in the adjacent GaAs becomes stronger and the large positive Grüneisen coefficient of LO mode results in its red Raman shift (Fig. 3). This interplay results in about 2% shift of the phonon energy with respect to its value in the bulk material. It agrees with the estimation that could be done from the experimental Raman spectra reported in [7]. Note that the obtained strain profiles and the red Raman shift of GaAs LO phonon in MQW could be explained on an atomistic scale only.

#### Acknowledgements

The work described in this publication was carried out at the Jet Propulsion Laboratory, California Institute of Tech-

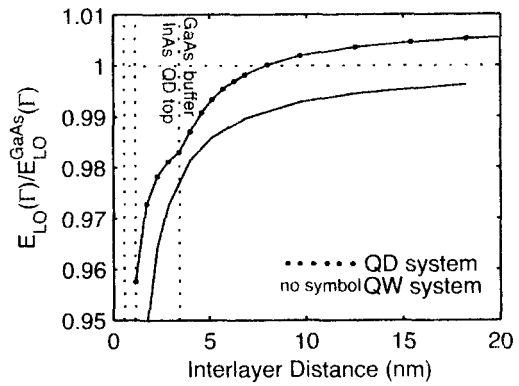


**Fig. 3.** Raman shift of the peak associated with the LO phonon in GaAs normalized to its energy in the bulk material as a function of the interlayer distance in InAs/GaAs MQW and semi-spherical SQD (lines marked with dots) structures. The vertical dotted lines mark the width of WL, QW, and the top of QD on WL. Note that the layers of QD on WL become separated at the distances larger than the third vertical dotted line.

Space Administration. Funding was provided under grants from ARDA, ONR, JPL, and NASA. This work was performed while one of the authors (O.L.L.) held a National Research Council Research Associateship Award at JPL.

#### References

- [1] P.N. Keating, *Phys. Rev.* **145**, 2, 637 (1966).
- [2] R.M. Martin, *Phys. Rev. B* **1**, 4005 (1970).
- [3] O.L. Lazarenkova, P. von Allmen, S. Lee, F. Oyafuso, and G. Klimeck, accepted in *Superlattices and Microstructures* (2004).
- [4] C. Pryor, J. Kim, L.W. Wang, A.J. Williamson, and A. Zunger, *J. Appl. Phys.* **83**, 2548 (1998).
- [5] F. Cerdeira, C.J. Buchenauer, F.H. Pollak, and M. Cardona, *Phys. Rev. B* **5**, 580 (1972).
- [6] Landolt-Börnstein, Series III, Vol. 17a *Intrinsic properties of group IV elements, III-V, II-VI, and I-VII compounds* (Berlin: Springer) 1987.
- [7] J. Ibáñez, A. Patané, M. Henini, L. Eaves, S. Hernández, R. Cuscó, L. Artús, Yu.G. Musikhin, and P.N. Brounkov, *Appl. Phys. Lett.* **83**, 3069 (2003).